BIOCHEMISTRY
including biophysical chemistry & molecular biology
Article

Biochemistry **2009,** *48,* 11961–11970 11961
DOI: 10.1021/bi901091v

Competition between $Co(NH_3)_6^{3+}$ and Inner Sphere Mg^{2+} Ions in the HDV Ribozyme†

Bo Gong,‡ Jui-Hui Chen,§ Philip C. Bevilacqua,*,∥ Barbara L. Golden,*,§ and Paul R. Carey*,‡

‡*Department of Biochemistry, Case Western Reserve University, 10900 Euclid Avenue, Cleveland, Ohio 44106,* §*Department of Biochemistry, Purdue University, 175 South University Street, West Lafayette, Indiana 47907, and* ∥*Department of Chemistry, The Pennsylvania State University, 104 Chemistry Building, University Park, Pennsylvania 16802*

Received July 2, 2009; Revised Manuscript Received October 6, 2009

ABSTRACT: Divalent cations play critical structural and functional roles in many RNAs. While the hepatitis delta virus (HDV) ribozyme can undergo self-cleavage in the presence of molar concentrations of monovalent cations, divalent cations such as Mg^{2+} are required for efficient catalysis under physiological conditions. Moreover, the cleavage reaction can be inhibited with $Co(NH_3)_6^{3+}$, an analogue of $Mg(H_2O)_6^{2+}$. Here, the binding of Mg^{2+} and $Co(NH_3)_6^{3+}$ to the HDV ribozyme is studied by Raman microscopic analysis of crystals. Raman difference spectra acquired at different metal ion conditions reveal changes in the ribozyme. When Mg^{2+} alone is introduced to the ribozyme, inner sphere coordination of $Mg(H_2O)_x^{2+}$ ($x \leq 5$) to nonbridging PO_2^- oxygen and changes in base stretches and phosphodiester group conformation are observed. In addition, binding of Mg^{2+} induces deprotonation of a cytosine assigned to the general acid C75, consistent with solution studies. When $Co(NH_3)_6^{3+}$ alone is introduced, deprotonation of C75 is again observed, as are distinctive changes in base vibrational ring modes and phosphodiester backbone conformation. In contrast to Mg^{2+} binding, $Co(NH_3)_6^{3+}$ binding does not perturb PO_2^- group vibrations, consistent with its ability to make only outer sphere contacts. Surprisingly, competitive binding studies reveal that $Co(NH_3)_6^{3+}$ ions displace some inner sphere-coordinated magnesium species, including ions coordinated to PO_2^- groups or the N7 of a guanine, likely G1 at the active site. These observations contrast with the tenet that $Co(NH_3)_6^{3+}$ ions displace only outer sphere magnesium ions. Overall, our data support two classes of inner sphere Mg^{2+}–PO_2^- binding sites: sites that $Co(NH_3)_6^{3+}$ can displace and others it cannot.

Metal ions play essential roles in the structure and function of ribozymes. Effects of metal ions on the small nucleolytic HDV[1] ribozyme (Figure 1) have been studied for a number of years (*1*–*9*). Self-cleavage of the HDV ribozyme has only a weak dependence on divalent ion identity. For instance, self-cleavage is efficient in the presence millimolar amounts of Mg^{2+}, Ca^{2+}, Mn^{2+}, Sr^{2+}, Ba^{2+}, or Co^{2+} (*1*, *5*). In addition, self-cleavage can occur in the complete absence of divalent cations if molar concentrations of monovalent cations such as Na^+, Li^+, and NH_4^+ are provided (*3*, *4*, *6*, *10*, *11*). Nonetheless, the reaction catalyzed in the presence of 1 M monovalent cations alone is 25–100-fold less efficient (*4*–*6*) and when extrapolated to physiological monovalent concentrations (~150 mM ionic strength) is ~500-fold less efficient (*4*). These observations suggest critical structural and functional roles for divalent cations in the ribozyme (*3*, *6*).

The catalytic activity of the HDV ribozyme is inhibited by competition of $Co(NH_3)_6^{3+}$ ions for Mg^{2+} ions (*3*). $Co(NH_3)_6^{3+}$ mimics hexhydrated Mg^{2+} in its size and coordination geometry and is exchange-inert ($k_{exchange,NH_3}$ ~10^{-10} s^{-1}); as such, it can make only outer sphere interactions with RNA (*2*, *12*–*14*). On the basis of these characteristics, it was initially suggested that the catalytic Mg^{2+} ion bound within the HDV ribozyme active site is in the hexahydrated form. Recent Raman crystallographic and biochemical studies, however, indicate that this ion is directly coordinated to the N7 of the cleavage site guanosine as an inner sphere ion and that it is likely only penta- or tetracoordinated to water molecules (*9*).

For several decades, Raman spectroscopy has provided invaluable insights into interactions between metal ions and nucleic acids (*15*–*21*). The ability of Raman to probe metal–nucleic acid interactions is further enabled by Raman *difference* spectroscopy (*21*, *22*). In this approach, the spectrum of the RNA without metal ions is subtracted from the spectrum of RNA with metal ions. Features in the difference spectrum provide detailed information on metal ion binding sites, changes in base stacking interactions, and backbone conformational changes owing to metal ion binding. This approach is particularly powerful when single crystals are used since Raman of single RNA or protein crystals provides data of unprecedented quality owing to high sample concentration in crystals, low background interference, and high spectral resolution (*8*, *23*–*25*).

Although we have not previously published data on cobalt hexamine binding to HDV, in order to understand the data and discussion in the present paper, we must summarize the findings

†This project was supported by NSF Grant MCB-0527102 (P.C.B.), the Purdue University Department of Biochemistry and Cancer Center (B.L.G.), and NIH Grant GM-54072 (P.R.C.).

*To whom correspondence should be addressed. P.R.C.: tel, (216) 368-0031; fax, (216) 368-3419; e-mail, prc5@cwru.edu. B.L.G.: tel, (765) 496-6165; fax, (765) 494-7897, e-mail, barbgolden@purdue.edu. P.C.B.: tel, (814) 863-3812; fax, (814) 863-8403; e-mail, pcb@chem.psu.edu.

[1]Abbreviations: HDV, hepatitis delta virus; $Mg(H_2O)_x^{2+}$ ($x \leq 5$), inner sphere Mg hydrate; –O–P–O–, phosphodiester back-bond; PO_2^-, phosphodioxy group; $K_{i,app}$, apparent binding constant of $Co(NH_3)_6^{3+}$; $K_{i,Co(NH_3)_6^{3+}}$, apparent inhibition constant of $Co(NH_3)_6^{3+}$; $K_{D,Mg^{2+}}$, apparent dissociation constant of Mg^{2+}; n or n_{Hill}, Hill coefficient; C75, cytosine residue at position 75 of the genomic HDV ribozyme; C75U, cytosine-to-uracil mutation at position 75 of the genomic HDV ribozyme.

Published on Web 11/04/2009

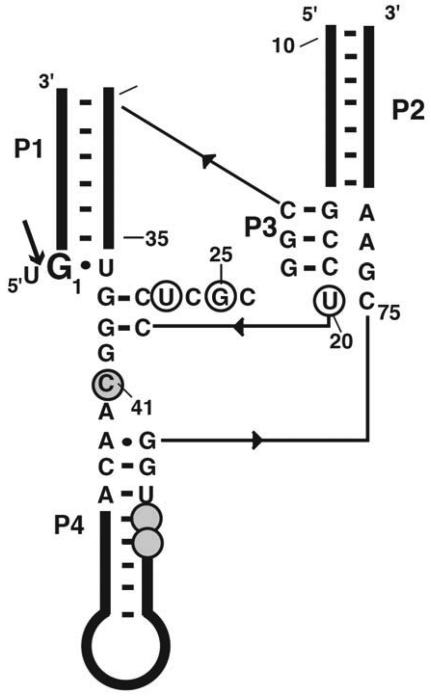

FIGURE 1: Secondary structure of the genomic HDV ribozyme. The RNAs used in this study are a 62 nt ribozyme annealed to a 9 nt inhibitor strand containing a methoxyuridine at position −1 to prevent cleavage. The ribozyme cleavage site is indicated with an arrow. Nucleotides involved in binding $Co(NH_3)_6^{3+}$ ion 1 (Figure 6A) are circled, and nucleotides involved in binding $Co(NH_3)_6^{3+}$ ion 2 (Figure 6C) are circled and shaded.

of three recent publications from our laboratories. In Gong et al. (*8*) we provided the first evidence for a direct relationship between the magnesium hydrate binding inner sphere to the oxygens of $-PO_2^-$ backbone groups and the upshift in the Raman symmetrical stretching frequency of these groups. This involved titrating Mg^{2+} hydrate into single crystals of the HDV ribozyme and identifying the Raman mode of bound magnesium penta- or tetrahydrate using isotopic substitutions. There is a simple linear relationship between the intensity of the upshifted (by 17 cm^{-1}) $-PO_2^-$ mode and the intensity of the magnesium penta- or tetrahydrate mode that appears near 320 cm^{-1}. This uniquely establishes that direct contact between the Mg^{2+} ion and the $-PO_2^-$ group brings about the observed upshift in the latter's Raman frequency. Other papers have dealt with the active site properties of HDV. In Gong et al. (*24*) we measured directly the pK_a of the active site cytosine 75 (C75) in crystals of HDV. This was made possible by the fact that we could identify the Raman feature from a single neutral cytosine in HDV, occurring near 1528 cm^{-1}. Its identity as C75 was confirmed by the finding that the variant of HDV possessing C75 replaced by uridine showed no evidence for a titration in the Raman spectra of the corresponding crystals. The results on the crystals received additional support from the observation that the crystal pK_a values obtained in the presence of 20 and 2 mM Mg^{2+}, 6.15 and 6.40, respectively, agree well with the values derived from HDV activity studies in solution. The active site studies were extended recently in Chen et al. (*9*) where solution kinetic and parallel Raman crystallographic studies examined the effects of pH on the rate and Mg^{2+} binding properties of wild-type and 7-deazaguanosine mutants of the HDV ribozyme. These data suggested that a previously unobserved hydrated magnesium ion interacts with N7 of the cleavage site G·U wobble base pair.

Herein, we use Raman crystallography to study interactions of Mg^{2+} and $Co(NH_3)_6^{3+}$ ions with the HDV ribozyme. These ions were chosen because of their unique physicochemical characteristics, spectrally disperse Raman features, and well-documented effects on HDV ribozyme function in solution. We find that introduction of either Mg^{2+} or $Co(NH_3)_6^{3+}$ results in deprotonation of a cytosine, previously identified as C75, as well as perturbation of the N7 of a guanine, previously identified as G1. C75 directly participates in catalysis, acting as the general acid in the cleavage reaction. Together, these data suggest that the binding sites of these two ions must be in proximity to C75 within the ribozyme active site and likely at least partially overlap. Moreover, these results indicate that inactivation of a ribozyme's activity by $Co(NH_3)_6^{3+}$ does not necessarily imply that the displaced Mg^{2+} ions were hexahydrated. Raman spectra also reveal that the molecular conformation of the HDV ribozyme in the presence of $Co(NH_3)_6^{3+}$ is slightly different from that in the presence of Mg^{2+}, which indicates that inhibition by $Co(NH_3)_6^{3+}$ could, in part, involve rearrangement of the active tertiary conformation.

MATERIALS AND METHODS

Chemicals. Chemicals used in the present study were purchased from Sigma. All stabilizing buffer solutions were prepared using 50 mM sodium cacodylate adjusted to the appropriate pH using HCl. Both Mg^{2+} and $Co(NH_3)_6^{3+}$ binding experiments were therefore performed in the presence of 50 mM Na^+ ions. Experiments were conducted at pH 6.0, except for competitive binding experiments between Mg^{2+} and $Co(NH_3)_6^{3+}$, which were at pH 7.0 to allow comparison with previous experiments in solution (*3*).

Preparation and Crystallization of the HDV Ribozyme. HDV ribozyme crystals used for Raman crystallography studies were prepared as described (*9*, *26*). For the present study, the cleavage reaction was inhibited by modifying the catalytic 2′-OH on the U-1 group to a 2′-OCH_3.

Raman Spectroscopy of HDV Ribozyme Crystals. Raman spectra were nonresonant and obtained at room temperature (22 °C) as described (*25*, *26*). All bound Mg^{2+} ions in the original HDV ribozyme crystals were removed by soaking in 50 mM EDTA five times, as described in Gong et al. (*8*). Crystals were then transferred to 5 μL drops containing stabilizing buffer (50% MPD, 2 mM spermine in 50 mM sodium cacodylate buffer, pH 6.0) and washed with this buffer three to five times to remove the EDTA from the crystals. Spectra in the absence of Mg^{2+} were then obtained. To obtain Raman spectra of the HDV crystal with varying Mg^{2+} and $Co(NH_3)_6^{3+}$ concentrations, crystals were then soaked in 5 μL of stabilizing buffer containing the desired cation salt for three times over the course of 2 h to ensure that metal ion-binding equilibrium had been reached. Equilibrium was determined by recording Raman spectra at several different times following buffer exchange.

Raman difference spectra and data analysis were performed using GRAMS/32 software (Galactic Industries, Inc.). In general, data were treated by first subtracting out the buffer from each spectrum according to the equation (*25*):

$$\begin{aligned}&[\text{RNA crystal (2)}] - [\text{RNA crystal (1)}]\\ &\quad = \{[\text{RNA crystal (2)} + \text{buffer (2)}] - [\text{buffer (2)}]\}\\ &\qquad - \{[\text{RNA crystal (1)} + \text{buffer (1)}] - [\text{buffer (1)}]\}\end{aligned}$$

Binding Analysis of Mg^{2+} in HDV Ribozyme Crystals. Mg^{2+} binding experiments were performed at pH 6.0 at concentrations of Mg^{2+} ranging from 0 to 30 mM. Standardized

Raman intensity of the neutral cytosine band at 1528 cm^{-1}, assigned to C75, was plotted as a function of Mg^{2+} concentration. The Hill coefficient was obtained by fitting to a Hill-type equation (eq 1; see Supporting Information for derivation):

$$\frac{I_{obs}}{I_{IS}} = \frac{I_0}{I_{IS}} + \left(\frac{I_{max}}{I_{IS}} - \frac{I_0}{I_{IS}}\right)\frac{[Mg^{2+}]^n}{K^n_{D,Mg^{2+}} + [Mg^{2+}]^n} \quad (1)$$

where I_{obs} is the observed intensity at 1528 cm^{-1}, I_{IS} is the intensity of an internal standard band at 725 cm^{-1}, which represents an adenine ring mode that is insensitive to metal binding in HDV, I_0 is the intensity of the 1528 cm^{-1} band at 0 mM Mg^{2+}, I_{max} is the intensity of the 1528 cm^{-1} band at saturating Mg^{2+}, n is Hill coefficient, and $K_{D,Mg^{2+}}$ is the concentration of Mg^{2+} corresponding to half-occupation of the Mg^{2+} binding sites in the ribozyme.

Analysis of $Co(NH_3)_6^{3+}$ Binding in HDV Ribozyme Crystals. Competitive binding of $Co(NH_3)_6^{3+}$ (0−1 mM) in the presence of 0−5 mM Mg^{2+} at pH 7.0 was studied using Raman crystallography. The standardized intensity of the band at 441 cm^{-1}, representing the Co−N stretching of $Co(NH_3)_6^{3+}$, was plotted as function of $Co(NH_3)_6^{3+}$ concentration and fit to eq 2 (see Supporting Information for derivation):

$$\frac{I_{obs}}{I_{IS}} = \frac{I_{max}}{I_{IS}}\left(\frac{[Co(NH_3)_6^{3+}]^n}{K^n_{i,app} + [Co(NH_3)_6^{3+}]^n}\right) \quad (2)$$

where I_{obs} is the observed intensity at 441 cm^{-1}, I_{IS} is the intensity of the internal standard band at 725 cm^{-1}, I_{max} is the intensity of the 441 cm^{-1} band at saturating $Co(NH_3)_6^{3+}$, n is the Hill coefficient for $Co(NH_3)_6^{3+}$ binding, and $K_{i,app}$ is the concentration of $Co(NH_3)_6^{3+}$ corresponding to half-occupation of the $Co(NH_3)_6^{3+}$ binding sites. This equation is essentially identical to eq 1, but with $I_0 = 0$, which is the case at 441 cm^{-1} (see Figure 7A).

The $Co(NH_3)_6^{3+}$ inhibition constant $K_{i,Co(NH_3)_6^{3+}}$ and the Mg^{2+} dissociation constant $K_{D,Mg^{2+}}$ were determined by a secondary plot of $K^n_{i,app}$ versus $[Mg^{2+}]^n$ (n fixed to 1.5 or 2, as appropriate) and fitting to eq 3 (see Supporting Information for derivation):

$$K^n_{i,app} = K^n_{i,Co(NH_3)_6^{3+}}\left(1 + \frac{[Mg^{2+}]^n}{K^n_{D,Mg^{2+}}}\right) \quad (3)$$

Apparent binding constants of $Co(NH_3)_6^{3+}$ ($K_{i,app}$) in 0, 1, 2, 3, 4, and 5 mM Mg^{2+} were obtained by fitting $Co(NH_3)_6^{3+}$ titration data to eq 2. Initially, we allowed the value of n to float and fit all of the data individually. Fitting gave values for n between 1.2 and 1.6 (Table 2). Next, we fit all data forcing n = 1, 1.5, 2, or 3. Only n = 1.5 or 2 gave good fits to the data, supporting binding of at least two $Co(NH_3)_6^{3+}$ ions to the ribozyme. Data for n = 1.5 are provided in the Results, while data for n = 2 are in the Supporting Information.

RESULTS

Overview. The Results are divided into eight sections. The first four sections describe how Mg^{2+} alone (1) interacts with the phosphate groups and nucleotide bases of the ribozyme, (2) induces conformational changes within the RNA, (3) causes cytosine deprotonation, and (4) binds in a reversible manner. The next two sections describe how $Co(NH_3)_6^{3+}$ alone (5) interacts with the ribozyme and causes cytosine deprotonation and (6) induces unique conformational changes of the ribozyme.

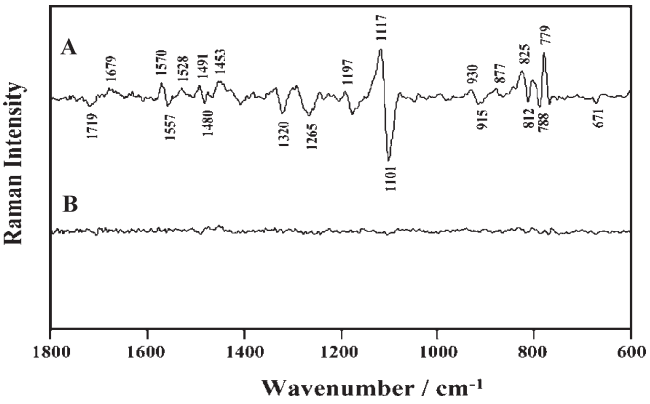

FIGURE 2: Effects of Mg^{2+} on HDV ribozyme conformation. (A) Raman difference spectrum of [HDV + 20 mM Mg^{2+}] minus [HDV no Mg^{2+}] (pH 6.0) was collected. [HDV no Mg^{2+}] condition was obtained by removing Mg^{2+} using 50 mM EDTA. The spectrum of the stabilization buffer was subtracted from each spectrum prior to subtraction (see Materials and Methods). Experimental details are described in Gong et al. (*8*). (B) Raman difference spectrum of [original crystal with 20 mM Mg^{2+}] minus [crystal resoaked in 20 mM Mg^{2+}] (pH 6.0). To obtain the spectrum of [crystal resoaked in 20 mM Mg^{2+}], a crystal of [HDV no Mg^{2+}] was resoaked in 20 mM Mg^{2+}-containing stabilization buffer after Mg^{2+} had been soaked out by EDTA.

The final two sections describe competition between Mg^{2+} and $Co(NH_3)_6^{3+}$ in (7) structural and (8) quantitative fashions.

Mg^{2+} Interactions with the HDV Ribozyme. The effect of Mg^{2+} on the HDV ribozyme was studied by recording Raman spectra of a ribozyme crystal in the presence and absence of Mg^{2+}. As described (*8*), the condition of [HDV no Mg^{2+}] was obtained by replacing the surrounding buffer containing 20 mM Mg^{2+} through five independent 50 mM EDTA soaks. This process "soaks out" the Mg^{2+} inside the solvent channels of the crystal. The resulting Raman difference spectrum of [HDV + Mg^{2+}] minus [HDV no Mg^{2+}] is shown in Figure 2A, where features above the baseline arise from [HDV + Mg^{2+}] and features below the baseline arise from [HDV no Mg^{2+}]. Importantly, the spectrum of the stabilization buffer was subtracted from each spectrum first, as described in the Materials and Methods. Spectral features were assigned on the basis of literature studies (*15*, *16*, *27*, *28*) and our recent work (*8*, *25*, *26*) and are provided in Table 1.

As shown in Figure 2A, the most intense differential band is centered near 1110 cm^{-1}.[2] The negative feature at 1101 cm^{-1}, which has been unambiguously assigned to symmetric stretching of PO_2^- (*27*, *28*), shifts to 1117 cm^{-1} owing to $Mg^{2+}-PO_2^-$ interactions. We recently assigned this differential spectral feature to inner sphere interactions between Mg^{2+} and PO_2^- groups on the basis of Mg hydrates bound to the HDV ribozyme, model compound studies, isotope effects, and quantum-mechanical calculations (*8*).

Differential bands are also observed near 1719, 1570/1557, 1491/1480, 1320, and 671 cm^{-1} (Figure 2A) and are likely due to effects of Mg^{2+} on the nucleobases. Importantly, these effects are not due simply to changes in ionic strength, as a Raman difference spectrum of [300 mM Na^+] minus [50 mM Na^+] does not show these features (data not shown). The negative band at 1719 cm^{-1} is assigned to the stretching vibrations of the carbonyl

[2]Differential bands are of special interest in the Raman because they generally mark where molecular features of metal-free RNA have been converted to features of metal-bound RNA.

Table 1: Positions (cm^{-1}) and Assignment of Raman Difference Bands Observed in Raman Difference Spectra of [HDV + Mg^{2+}] minus [HDV No Mg^{2+}][a]

wavenumber/cm^{-1}	assignment
1719	C=O
1679	C=O
1570/1557	G (A?)
1528	C
1491/1480	G
1453	C−H deformation
1320	G
1265 (broad)	C^+
1197	G
1117/1101	PO_2^-
930/915	ribose backbone
877	ribose backbone
825/812	−O−P−O−
779	C (U?)
788	C^+ (U?)
671	G

[a]C, neutral cytosine; C^+, protonated cytosine; C=O, carbonyl group. The features assigned to the bases are due to ring modes.

groups of G, C, and U involved in interbase hydrogen bonds (*27*−*29*). The intensity loss of this band likely reflects subtle change in interbase hydrogen binding interactions in the presence of Mg^{2+}. The differential band at 1570/1557 cm^{-1} is attributed to G ring modes with possibility of minor contribution from A and represents perturbations of purines upon Mg^{2+} binding, the details of which are not yet understood. These changes are also consistent with the observation of negative bands at 1320 and 671 cm^{-1}, as these two bands have been unambiguously assigned to ring breathing of G bases. The intensity decrease of these two bands in the presence of Mg^{2+} may also indicate alteration of G stacking (*30*, *31*).

The differential band at 1491/1480 cm^{-1} is assigned mainly to a G mode with a strong component from N7−C8 vibrational motion (*16*, *32*). Previous Raman studies showed that the band perturbation at this region indicates binding of electrophilic agents (Mg^{2+} in this case) at N7 of G (*16*, *33*). In our recent work, we observed a similar spectral feature in the pH difference spectrum of [HDV pH 7.5] minus [HDV pH 5.0] (*9*). This feature is lost upon site-specific mutation at N7 of G1 using 7-deaza substitution, supporting the conclusion that the band perturbation near 1485 cm^{-1} results, at least in part, from an inner sphere contact between the active site Mg^{2+} and the N7 of G1 (*9*).

Mg^{2+} Binding Induces Ribozyme Conformational Changes. The differential feature observed at 825/812 cm^{-1} in Figure 2A can be assigned to symmetric stretches of phosphodiester backbone modes (−O−P−O−), which are sensitive to conformational changes (*27*, *28*). The negative band of 812 cm^{-1} resulting from canonical A-form RNA shifts to higher frequency (825 cm^{-1}) in the presence of Mg^{2+}. In other nucleic acids, this kind of shift has been considered an indicator of conformational changes upon Mg^{2+} binding, where canonical A-type C3′-endo-anti ribose puckers change to C2′-endo-anti (*34*).

The nonhelical regions of HDV (bulge, loop, etc.) are likely candidates for generating these conformational perturbations (*34*, *35*). A semiquantitative analysis on the basis of band intensity decrease of −O−P−O− indicates that the deviation is ~3% the intensity of the peak in the parent spectrum, suggesting that the conformational change is small. These changes may be localized to C41 and C75, or they may represent small effects spread over the entire ribozyme (see Discussion).

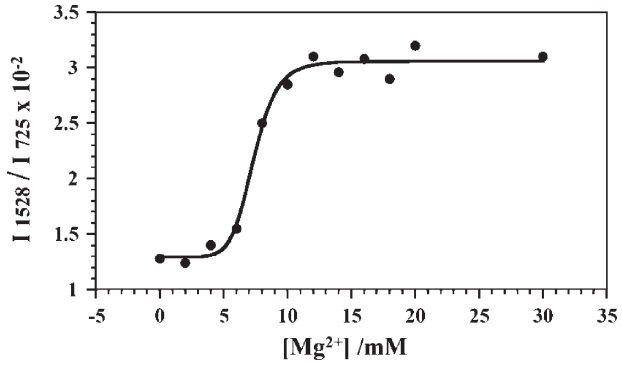

FIGURE 3: Dependence of C75 ionization on Mg^{2+} concentration. HDV crystals at pH 6.0 show a Mg^{2+} concentration-dependent change of Raman intensity of the neutral C75 peak (1528 cm^{-1}). The *y*-axis is the ratio of Raman intensity of neutral C75 at 1528 cm^{-1} to the intensity of the adenine ring mode at 725 cm^{-1} (internal standard). The intensity of the latter is independent of Mg^{2+} concentration.

Mg^{2+} Binding Induces Cytosine Deprotonation. Raman Mg^{2+} difference spectra reveal features that arise from neutral and protonated cytosine, including a positive band at 1528 cm^{-1}, a negative band at 1265 cm^{-1}, and a differential band at 788/779 cm^{-1} (Figure 2A). These spectral features are readily assigned on the basis of work of ourselves (*9*) and others (*27*). The negative 1265 cm^{-1} band has been assigned to protonated cytosine, indicating that cytosine deprotonates at pH 6.0 when Mg^{2+} is added. Complementarily, the positive 1528 cm^{-1} band denotes the presence of additional neutral cytosine in the presence of 20 mM Mg^{2+}.

We previously demonstrated that there is just a single cytosine base that is protonatable in this pH range and assigned it as the catalytic cytosine (C75) on the basis of mutational analysis (*26*). The Raman difference spectrum of [HDV + Mg^{2+}] minus [HDV no Mg^{2+}] (Figure 2A) thus provides strong evidence that addition of 20 mM Mg^{2+} leads to the deprotonation of C75.

The extent of cytosine deprotonation can be quantitated via the absolute intensity of the 1528 cm^{-1} band in the Raman difference spectrum. Using band integrations as previously described (*26*), we determined that exposing the pH 6.0 crystal to 20 mM Mg^{2+} creates a population increase of neutral cytosine of about 10 mM. Since pH 6.0 is slightly below the pK_a value of 6.15, previously identified by Raman crystallography under these Mg^{2+} conditions, and because the concentration of HDV ribozyme in the crystal is about 26 mM (*26*), it appears that adding Mg^{2+} at constant pH drives deprotonation of a single cytosine, the active site cytosine residue (C75).[3] This interpretation is consistent with solution kinetics and Raman crystallographic data, which demonstrated that the pK_a of C75 is inversely correlated with Mg^{2+} concentration (*3*, *26*).

To semiquantitatively analyze the relationship of Mg^{2+} binding and C75 protonation, we measured the standardized intensity

[3]The fraction of deprotonated cytosine, assuming a simple single protonation event, can be calculated as $f = 10^{pH-pK_a}/(1 + 10^{pH-pK_a})$, which gives a value of 0.41 using a pH of 6.0 and a pK_a of 6.15. Given that the concentration of RNA in the crystal is 26 mM, approximately 10.7 mM would deprotonate upon raising the Mg^{2+} concentration, consistent with the data herein. These calculations assume that the pK_a for C75 in the absence of Mg^{2+} is significantly elevated, consistent with an experimental pK_a of 7.25 extrapolated to no bound Mg^{2+} from pH-dependent Mg^{2+} binding experiments in solution (*42*).

Table 2: Comparison of Binding Parameters from Raman Crystallographic and Biochemical Studies[a]

condition	Raman crystallographic			biochemical		
	$K_{D,Mg^{2+}}$ (mM)	$K_{i,Co(NH_3)_6^{3+}}$ (μM)	n_{Hill}	$K_{D,Mg^{2+}}$ (mM)	$K_{i,Co(NH_3)_6^{3+}}$ (μM)	n_{Hill}
Mg^{2+} alone[b]	7.4 ± 0.2		8.0 ± 1.6	9.8[c]		1.3
competitive binding of $Co(NH_3)_6^{3+}$ and Mg^{2+}[d]	1.7 ± 0.4	47 ± 9	1.5[e]	2.4[f]	45 ± 10	1.4[g]
	2.0 ± 0.3	54 ± 8	2[h]			

[a]The HDV single crystal used in this study has 2′-OCH_3 substitution on the U-1 group. [b]Mg^{2+}−HDV interaction was studied at pH 6.0. [c]Value measured at pH 6.0 (*3*). [d]Competitive binding of $Co(NH_3)_6^{3+}$ and Mg^{2+} was performed at pH 7.0. [e]The n_{Hill} for both $Co(NH_3)_6^{3+}$ and Mg^{2+} binding was held constantly at 1.5 for all analyses (see text) since the floating values of n_{Hill} in the presence of 0, 1, 2, 3, 4, and 5 mM Mg^{2+} are 1.4 ± 0.2, 1.4 ± 0.3, 1.2 ± 0.3, 1.4 ± 0.4, 1.6 ± 0.2, and 1.4 ± 0.2, respectively (average R^2 was 0.9814). [f]Value measured at pH 7.0 (*3*). [g]This value is for Mg^{2+} binding at pH 7.0 (*3*). The Hill value for $Co(NH_3)_6^{3+}$ was not measured explicitly in that study. [h]n_{Hill} = 2 also gave a good curve fit using eq 2 (Figure S1A; see Supporting Information) (average R^2 was 0.9844). However, n_{Hill} = 1 and n_{Hill} = 3 did not (data not shown) (average R^2 values were 0.9642 and 0.9544, respectively).

of the neutral C75 band at 1528 cm^{-1} as a function of added Mg^{2+} concentration. The ratios of the 1528 to 725 cm^{-1} intensities in the Mg^{2+} concentration range from 0 to 30 mM are plotted in Figure 3 and fit to eq 1. (The 725 cm^{-1} band, an adenosine ring mode, was chosen since it is insensitive to Mg^{2+} binding, as confirmed by the absence of the 725 cm^{-1} band in Figure 2A.)[4] Analysis gave a Hill coefficient of 8.0 ± 1.6 and a dissociation constant $K_{D,Mg^{2+}}$ of 7.4 mM for bound magnesium (Table 2). The latter value is in good agreement with biochemical studies at pH 6.0 ($K_{D,Mg^{2+}}$ ~9.8 mM) (*3*).

Binding of Mg^{2+} Is Reversible. As mentioned, the difference spectrum in Figure 2A was generated by treating a 20 mM Mg^{2+}-containing crystal with 50 mM EDTA five times and subtracting its Raman spectrum from that of the original crystal in the presence of 20 mM Mg^{2+}. Subsequently, we reexposed the EDTA-soaked crystal to a solution of 20 mM Mg^{2+} in order to "resoak in" Mg^{2+}. In this case, the crystal was soaked three times in the 20 mM Mg^{2+}-containing stabilization buffer. The difference spectrum of [original crystal with 20 mM Mg^{2+}] minus [crystal resoaked in 20 mM Mg^{2+}] is essentially flat (Figure 2B). Absence of hysteresis suggests that soaking Mg^{2+} in and out does not damage the crystals and that binding of Mg^{2+} is reversible.

$Co(NH_3)_6^{3+}$ Interactions with the HDV Ribozyme and Induction of Cytosine Deprotonation. Next, we turn our attention to the interactions of $Co(NH_3)_6^{3+}$ with the HDV ribozyme crystals. Effects of $Co(NH_3)_6^{3+}$ binding were revealed by the Raman difference spectrum of [HDV + 0.1 mM Co-$(NH_3)_6^{3+}$] minus [HDV no $Co(NH_3)_6^{3+}$] (Figure 4). An apparent concentration of 0.1 mM $Co(NH_3)_6^{3+}$ was established in the crystals by soaking them three times in 0.1 mM $Co(NH_3)_6^{3+}$-containing stabilization buffer. Intense positive bands observed in the spectral region 250—1800 cm^{-1} are due mainly to bound $Co(NH_3)_6^{3+}$, including N−H_3 bending near 1333 cm^{-1}, Co−N stretching at 491 and 441 cm^{-1}, and N−Co−N deformation at 315 cm^{-1}. These features are essentially unchanged compared to the corresponding modes seen for the unbound cobalt hexamine. Importantly, these signals arise from bound rather than free $Co(NH_3)_6^{3+}$ because the Raman spectrum of the stabilization buffer is subtracted from the parent [HDV + 0.1 mM Co-$(NH_3)_6^{3+}$] spectrum (see Materials and Methods, "Raman Spectroscopy of HDV Ribozyme Crystals"). Thus, negative peaks from unbound $Co(NH_3)_6^{3+}$ do not appear in Figures 4 and 5.

[4]For pH titrations, we previously used the PO_2^- stretch at 1101 cm^{-1} to standardize the 1528 cm^{-1} stretch (*24*), but that was not used here because the 1101 cm^{-1} feature is sensitive to Mg^{2+} binding (Figure 2A).

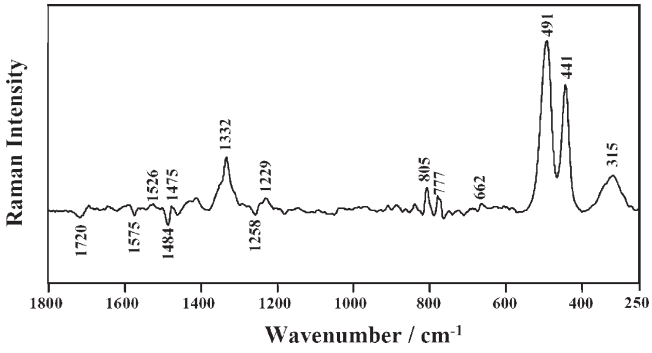

FIGURE 4: Effects of $Co(NH_3)_6^{3+}$ on HDV ribozyme conformation. Raman difference spectrum of [HDV + 0.1 mM $Co(NH_3)_6^{3+}$] minus [HDV no $Co(NH_3)_6^{3+}$] (pH 6.0) was collected. Both [HDV + 0.1 mM $Co(NH_3)_6^{3+}$] and [HDV no $Co(NH_3)_6^{3+}$] spectra were collected in the absence of added Mg^{2+}. The spectrum of the stabilization buffer was subtracted from each spectrum first. Main band assignments are provided in Table 1 except bands resulting from $Co(NH_3)_6^{3+}$: 1333 cm^{-1} (N−H_3 bending of $Co(NH_3)_6^{3+}$), 491 and 441 cm^{-1} (Co−N stretching of $Co(NH_3)_6^{3+}$), and 315 cm^{-1} (N−Co−N deformation of $Co(NH_3)_6^{3+}$).

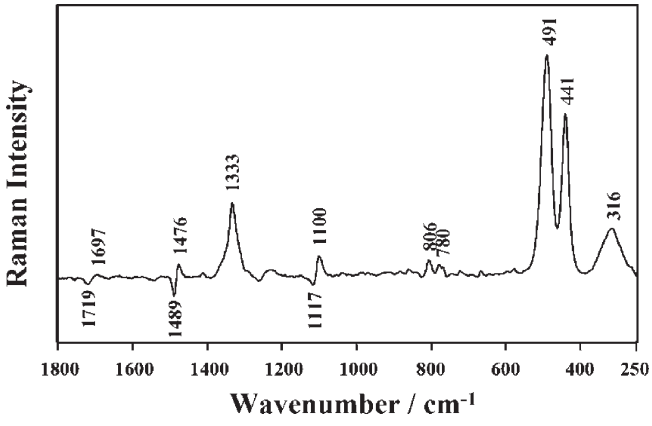

FIGURE 5: Competitive binding of Mg^{2+} and $Co(NH_3)_6^{3+}$ in the HDV ribozyme. Raman difference spectrum of [HDV + 20 mM Mg^{2+} + 5 mM $Co(NH_3)_6^{3+}$] minus [HDV + 20 mM Mg^{2+}] at pH 7.0 was collected. The spectrum of the stabilization buffer was subtracted from each spectrum first. The differential peak around 1100 cm^{-1} directly indicates the loss of inner sphere bound Mg^{2+} upon Co-$(NH_3)_6^{3+}$ binding. Band assignments are described in Table 1 and the caption of Figure 4.

Binding of $Co(NH_3)_6^{3+}$ also perturbs several vibrational modes of the HDV ribozyme. The differential band of 1484/1475 cm^{-1} in Figure 4 represents perturbation of one or more

guanine ring modes upon $Co(NH_3)_6^{3+}$ binding. The guanine base(s) is in an environment in the absence of $Co(NH_3)_6^{3+}$ that gives rise to the band of frequency of 1484 cm^{-1}, which is similar to the frequency of guanine ring in aqueous GTP (*27*). In the presence of $Co(NH_3)_6^{3+}$ this band is reduced in intensity and/or shifts providing a less intensity feature at 1475 cm^{-1}. A similar effect gives rise to a negative band at 1575 cm^{-1}, which is due to guanine or possibly adenine (Table 1). The negative band at 1720 cm^{-1} indicates modest perturbation to interbase hydrogen bonding in the presence of the metal ions, while the positive band at 777 cm^{-1} is assigned to C and/or U and indicates a small change in the environment of these bases.

While binding of $Co(NH_3)_6^{3+}$ perturbs a number of vibrational modes of the ribozyme, it does not perturb PO_2^- bands of the ribozyme. In contrast to Mg^{2+} binding, which gives a strong PO_2^- differential band near 1100 cm^{-1} (Figure 2A), the Raman stabilization buffer-corrected difference spectrum of [HDV + $Co(NH_3)_6^{3+}$] minus [HDV no $Co(NH_3)_6^{3+}$] does not show peak perturbations in this region. This observation is consistent with our recent work that supported the ~20 cm^{-1} upshift of the 1100 cm^{-1} PO_2^- peak as being due to inner sphere interactions with Mg^{2+} (*8*). Thus, as expected, $Co(NH_3)_6^{3+}$ does not form inner sphere interactions with the ribozyme.

While many of the above features are expected when most RNAs are exposed to $Co(NH_3)_6^{3+}$, one feature is unique to the HDV ribozyme. Deprotonation of C75 is induced when $Co(NH_3)_6^{3+}$, like Mg^{2+}, is soaked into HDV ribozyme crystals. Evidence of cytosine deprotonation includes spectral features at 1526, 1258, and 777 cm^{-1} (Figure 4), as described above for Mg^{2+}. This observation suggests that $Co(NH_3)_6^{3+}$, like the $Mg(H_2O)_5^{2+}$ coordinated to the N7 of G1, binds in the active site close enough to C75 that it exhibits electrostatic repulsion with the bound proton.

$Co(NH_3)_6^{3+}$ Binding Induces Ribozyme Conformational Changes. For Mg^{2+} binding, a positive differential band is observed at 825 cm^{-1} (Figure 2A), while for $Co(NH_3)_6^{3+}$ binding, a positive differential band is observed at 805 cm^{-1} (Figure 4). These differences support the appearance of slightly more canonical A-type RNA structures in the presence of $Co(NH_3)_6^{3+}$. The estimated change of intensity of the −O−P−O− band at 805 cm^{-1} is ~2% of the parent band, which suggests that the main increase of canonical A-type RNA conformation (which has a 3′-endo sugar pucker) is very small.

Overall, comparison of the differential bands located at the −O−P−O− region in Figures 2A and 4 provides spectroscopic evidence that small conformational changes are induced by both $Co(NH_3)_6^{3+}$ and Mg^{2+} binding but that the nature of these conformational changes is different: Mg^{2+} induces an *increase* in the mean amount of C2′-endo in the sugar backbone, while $Co(NH_3)_6^{3+}$ induces a *decrease*. These conformations are discussed in detail under "Mg^{2+} Binding Induces Ribozyme Conformational Changes" above.

Competitive Binding of $Co(NH_3)_6^{3+}$ and Mg^{2+}: Structural Analysis. Now that the separate effects of Mg^{2+} and $Co(NH_3)_6^{3+}$ have been presented, we consider interactions between these ions. Competitive binding between $Co(NH_3)_6^{3+}$ and Mg^{2+} in HDV crystals can be probed using a Raman difference experiment: [HDV + Mg^{2+} + $Co(NH_3)_6^{3+}$] minus [HDV + Mg^{2+}], each with appropriate stabilization buffers subtracted (Figure 5). Most of the spectral features observed in this difference spectrum are similar to those for $Co(NH_3)_6^{3+}$ binding alone (Figure 4). Since the Raman spectrum of [HDV + Mg^{2+} + $Co(NH_3)_6^{3+}$] was recorded in the presence of 5 mM $Co(NH_3)_6^{3+}$ *and* 20 mM Mg^{2+}, this observation supports the binding affinity of $Co(NH_3)_6^{3+}$ being significantly higher than that of Mg^{2+}. This observation is consistent with solution experiments, which indicated ~50-fold tighter binding of $Co(NH_3)_6^{3+}$ (*3*). This observation is confirmed quantitatively in the crystal by analyzing the inhibition constant of $Co(NH_3)_6^{3+}$ ($K_{i,Co(NH_3)_6^{3+}}$) and the dissociation constant of Mg^{2+} ($K_{D,Mg^{2+}}$), as described below.

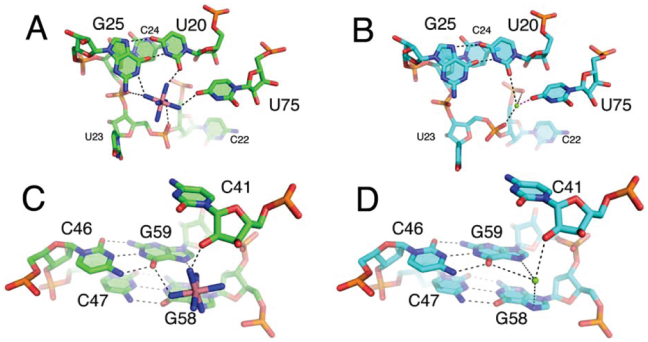

FIGURE 6: Cobalt hexamine binding sites in the HDV ribozyme overlap with Mg^{2+} binding sites. The crystal structure of the inactive C75U ribozyme bound to a substrate was determined in the presence of $Co(NH_3)_6^{3+}$ (PDB ID 1SJF, shown in green) and in the presence of Mg^{2+} (PDB ID 1SJ3, shown in blue) (*37*). $Co(NH_3)_6^{3+}$ ion near the active site (A) ("site 1") displaces a Mg^{2+} ion with an inner sphere ligand from U75 (B, highlighted in magenta). A second $Co(NH_3)_6^{3+}$ ion binds in the major groove of P4, near C41 (C) ("site 2"). This $Co(NH_3)_6^{3+}$ ion displaces a $Mg(H_2O)_6^{2+}$ ion bound to the RNA purely through second-shell ligands (D).

A significant feature of Figure 5 is the differential band of PO_2^- in the 1100 cm^{-1} region, which is characterized by the positive band at 1100 cm^{-1} with a trough at 1117 cm^{-1}. This differential is the inverse of that observed in Figure 2A for inner sphere Mg^{2+} binding. The trough at 1117 cm^{-1} indicates less Mg^{2+} coordinated to the PO_2^- oxygen in the presence of $Co(NH_3)_6^{3+}$. Similarly, the positive feature at 1100 cm^{-1} reflects the appearance of a new, unperturbed PO_2^- population. These observations comprise strong evidence that $Co(NH_3)_6^{3+}$ has displaced inner sphere Mg^{2+}−PO_2^- complexes in the HDV ribozyme.

Using the intensity of the 1100 cm^{-1} differential in Figure 5 relative to the parent peak at 1100 cm^{-1}, it is possible to assess that 1−1.5 Mg^{2+}−PO_2^- inner sphere contacts are displaced by $Co(NH_3)_6^{3+}$ (*8*). This value is consistent with crystallographic studies of the HDV ribozyme, in which one high-occupancy $Co(NH_3)_6^{3+}$ binding site that overlaps with an inner sphere bound Mg^{2+} was observed (Figure 6A,B); we note that a second $Co(NH_3)_6^{3+}$ binding site was also observed, but it overlaps with an outer sphere bound Mg^{2+} ion (Figure 6C,D). We also note that the number of Mg^{2+} ions displaced is less than 5 (*8*), the number of Mg^{2+} ions observed in the absence of $Co(NH_3)_6^{3+}$, indicating that $Co(NH_3)_6^{3+}$ cannot effectively displace all of the Mg^{2+} ions (see Discussion).

A further observation in the competition difference spectrum is the differential near 1489/1476 cm^{-1} (Figure 5). As observed from inspection of Figures 2A and 4, Mg^{2+} and $Co(NH_3)_6^{3+}$ ions give rise to differentials with opposite signs in this region, with the differential in Mg^{2+} being characteristic of coordination to the N7 of G1. Thus, the data in Figure 5 support the ability of a $Co(NH_3)_6^{3+}$ ion to displace the catalytic inner sphere Mg^{2+} ion at the N7 of G1.

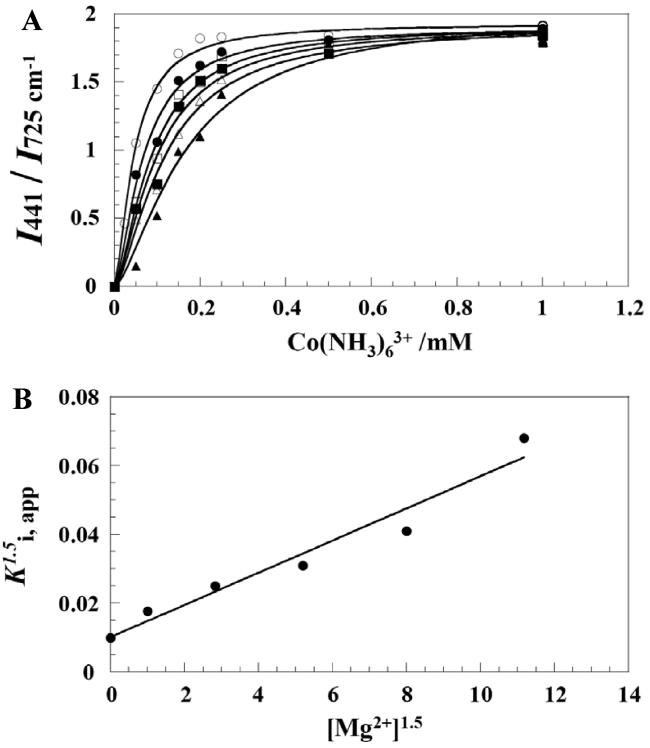

FIGURE 7: Quantitative assessment of competition between $Co(NH_3)_6^{3+}$ and Mg^{2+}. (A) $Co(NH_3)_6^{3+}$ binding profiles in HDV ribozyme at Mg^{2+} concentrations of 0 mM (○), 1 mM (●), 2 mM (□), 3 mM (■) 4 mM (△), and 5 mM (▲). The *y*-axis is the ratio of Raman intensity of Co−N stretching of $Co(NH_3)_6^{3+}$ at 441 cm^{-1} to the intensity of the adenine ring mode at 725 cm^{-1} (internal standard). Data were fit to eq 2, from which the apparent binding constants of $Co(NH_3)_6^{3+}$ ($K_{i,app}$) were obtained in the presence of different $[Mg^{2+}]$. All experiments were performed at pH 7.0. (B) Secondary plot of $K^{1.5}_{i,app}$ versus $[Mg^{2+}]^{1.5}$ fit to eq 3. This gave values of 47 μM and 1.7 mM for $K_{i,Co(NH_3)_6^{3+}}$ and $K_{D,Mg^{2+}}$, respectively.

Competitive Binding of $Co(NH_3)_6^{3+}$ and Mg^{2+}: Quantitative Analysis. Lastly, a quantitative analysis of competition between $Co(NH_3)_6^{3+}$ and Mg^{2+} was performed. This was achieved by measuring the intensity ratio of the Co−N stretching band at 441 cm^{-1} referenced to 725 cm^{-1} (the same internal standard used in Figure 3) as a function of $Co(NH_3)_6^{3+}$ concentration. This titration was carried out in the background of 0, 1, 2, 3, 4, or 5 mM Mg^{2+} at pH 7.0 (Figure 7A).

Fitting the $Co(NH_3)_6^{3+}$ titration data to eq 2 using a Hill coefficient of 1.5 (see Materials and Methods) gave $K_{i,app}$s for $Co(NH_3)_6^{3+}$ of 0.046, 0.069, 0.085, 0.099, 0.119, and 0.167 mM, respectively. A secondary plot of $K^{1.5}_{i,app}$ versus $[Mg^{2+}]^{1.5}$ (Figure 7B) using eq 3 afforded the apparent inhibition constant for $Co(NH_3)_6^{3+}$ ($K_{i,Co(NH_3)_6^{3+}}$) of 47 μM and the apparent dissociation constant of Mg^{2+} ($K_{D,Mg^{2+}}$) of 1.7 mM, respectively (Table 2). (This K_i is defined in eq 3 and is likely intermediate between the actual K_is for the two $Co(NH_3)_6^{3+}$ suggested from n_{Hill}.) These values are in agreement with previous biochemical results at pH 7.0 of 45 μM and 2.4 mM for $K_{i,Co(NH_3)_6^{3+}}$ and $K_{D,Mg^{2+}}$, respectively (*3*), as well as the Hill value of 1.4 for Mg^{2+}, suggesting that the conformation of the RNA in the crystal is catalytically relevant. In addition, the Hill constant of 1.5 supports binding of at least two $Co(NH_3)_6^{3+}$ ions in place of Mg^{2+} ions, consistent with spectral data presented above. A Hill coefficient of 2 also gave reasonable fits to the data, while Hill coefficients of 1 or 3 were less good, consistent with this interpretation (see Supporting Information).

DISCUSSION

Metal ions serve a variety of catalytic and structural roles in RNA. Divalent ions are particularly important as they can neutralize more charge with less entropy loss than monovalent ions. In the case of the HDV ribozyme, crystal structures have revealed the presence of many divalent metal ion binding sites (*36*, *37*). These include fully hydrated magnesium ions found in the major groove and a partially hydrated magnesium ion that bridges the close approach of the negatively charged RNA backbone. A metal ion also appears to be recruited to the active site in the presence of the inactivating C75U mutation (*37*).

$Co(NH_3)_6^{3+}$ has been used as a mechanistic probe in both protein and RNA enzymes. As Jou and Cowan pointed out, $Co(NH_3)_6^{3+}$ is similar in size to $Mg(H_2O)_6^{2+}$, Co^{3+} is slow to exchange its ligands, and $Co(NH_3)_6^{3+}$ can hydrogen bond similarly to $Mg(H_2O)_6^{2+}$ (*38*). In some cases, protein and RNA enzymatic activity has been shown to be retained when $Co(NH_3)_6^{3+}$ is added into the reaction, while in other cases activity it is lost. Retention of activity has been used to infer a functional role for fully hydrated metal ions that do not coordinate directly to macromolecular ligands in the reaction. Examples include the proteins RNase H and exonuclease III (*38*, *39*), as well as the hairpin ribozyme and an acyl-transferase ribozyme (*12*−*14*). In these instances, the inference was that the hydrated magnesium ion serves an electrostatic or structural role but does not participate in proton transfer. Loss of activity through inhibition of the competitive type has also been used to suggest a functional role for an outer sphere metal ion in an enzymatic reaction, but in a more active role wherein the ability of the metal ion to deprotonate is lost (*3*). This follows because $Co(NH_3)_6^{3+}$ is similar in size and charge to $Mg(H_2O)_6^{2+}$ but lacks exchangeable ligands and the ability to participate in proton transfer under physiologically relevant conditions. In the case of the HDV ribozyme, the inference was that a fully hydrated magnesium ion serves as a general base in the reaction. Our results in the present study serve as a paradigm shifter because they show that $Co(NH_3)_6^{3+}$ can compete for $Mg(H_2O)_{4,5}^{2+}$ sites, too. As such, retention of activity upon $Co(NH_3)_6^{3+}$ addition does not necessarily imply that the displaced magnesium was outer sphere bound (although they do show activity is at least compatible with an outer sphere coordination); likewise, loss of activity upon $Co(NH_3)_6^{3+}$ addition does not necessarily imply that the displaced magnesium was outer sphere bound. Apparently, the stronger Coulombic attractions and plasticity of the macromolecule allow the outer sphere trivalent ion to bind into inner sphere sites.

In the present study, we used Raman spectroscopic data to analyze the nature of Mg^{2+} ion interaction with the HDV ribozyme by studying Mg^{2+} binding, $Co(NH_3)_6^{3+}$ binding, and their competition. A key finding of our studies is that $Co(NH_3)_6^{3+}$, which binds in an outer sphere fashion, can displace several Mg^{2+} ions with inner sphere ligands, including the Mg^{2+} ion at G1. Importantly, the qualitative and quantitative results observed herein are fully consistent with solution data, supporting catalytic relevance of the interactions.

Nature of the Interactions between Metal Ions and RNA. The backbone of RNA is negatively charged, and many magnesium binding sites within folded RNAs involve direct coordination between divalent metal ions and nonbridging phosphate oxygens. Our earlier observations showed that inner sphere $Mg^{2+}-PO_2^-$ contacts in HDV give rise to a strong spectral

perturbation of the PO_2^- symmetric stretch peak near 1100 cm^{-1}, which take the form of a significant intensity loss of the PO_2^- peak combined with an ~20 cm^{-1} higher frequency shift (*8*). Similar effects have been noted in model compounds (Christian, Gong, and Carey, unpublished observations). The inner sphere nature of this ligand was confirmed by a positive correlation between the perturbation to the PO_2^- stretch and the appearance of a $Mg(H_2O)_x^{2+}$ ion ($x \leq 5$) mode near 320 cm^{-1}. The present work builds on these findings, and the data in Figure 2 show that the changes in HDV upon Mg^{2+} binding extend beyond the PO_2^- groups to include changes in base ring modes and in the conformation of the ribose groups within the backbone.

The changes brought about by $Co(NH_3)_6^{3+}$ binding in HDV crystals are markedly different than those observed upon Mg^{2+} ion binding. Since the cobalt complex cannot make inner sphere contact to the phosphate oxygens, no band perturbation near 1100 cm^{-1} is observed (Figure 4). Moreover, when 5 mM $Co(NH_3)_6^{3+}$ is allowed to compete with 20 mM Mg^{2+}, a 1117/1100 cm^{-1} differential is revealed in the Raman difference data (Figure 5). This feature was quantitated to show that $Co(NH_3)_6^{3+}$ displaces $Mg(H_2O)_x^{2+}$ ion ($x \leq 5$) at approximately 1−1.5 inner sphere PO_2^- sites in the HDV ribozyme.

RNAs attract a cloud of diffusely bound positive ions whose binding is weak (millimolar) and likely highly dynamic (*40*, *41*), and thus, it can be envisaged that $Co(NH_3)_6^{3+}$ can out-compete Mg^{2+} at these sites on an electrostatic basis. This contrasts with $Mg(H_2O)_x^{2+}$ ($x \leq 5$) ions that are bound within discrete electronegative binding pockets formed by the RNA and are often visible in X-ray crystal structures. Thus, competition between $Mg(H_2O)_x^{2+}$ and $Co(NH_3)_6^{3+}$ may occur at 1−2 individual sites or may result from the mean of lower occupancies at more sites. Previous studies have suggested that there are 5−6 Mg^{2+} ions within the HDV ribozyme that coordinate to $-PO_2^-$ and could contribute to this differential (*8*). Our finding that $Co(NH_3)_6^{3+}$ can displace $Mg(H_2O)_x^{2+}$ with inner sphere contacts at the oxygens of PO_2^- is at variance with the generally stated view that $Co(NH_3)_6^{3+}$ can only displace Mg^{2+} at outer sphere sites, although it is also clear that $Co(NH_3)_6^{3+}$ cannot displace all inner sphere Mg^{2+} ions.

Raman difference spectra also reveal metal-dependent changes in the bases. In competition experiments between Mg^{2+} and $Co(NH_3)_6^{3+}$ a differential band corresponding to the guanosine base is observed around 1480 cm^{-1} (Figure 5). The negative limb at 1489 cm^{-1} is likely due to release of Mg^{2+} bound at the N7 of G (*9*) while the positive limb at 1476 cm^{-1} is assigned to G free from any strong direct interaction with a metal. These data suggest that $Co(NH_3)_6^{3+}$ can displace a $Mg(H_2O)_x^{2+}$ ion that makes an inner sphere contact to the N7 of a guanosine. In addition, at least two Mg^{2+} ions are displaced as suggested by the Hill coefficient of 1.5 for $Co(NH_3)_6^{3+}$ competition with Mg^{2+} ions bound (Figure 7). Thus, it is likely that at least one Mg^{2+} ion at an inner sphere complex with PO_2^- is displaced. As Mg^{2+} ions rarely make simultaneous contact to an N7 and a nonbridging phosphate oxygen, the $Mg(H_2O)_x^{2+}$ ion displaced from the N7 of G is likely distinct from the ion(s) displaced at nonbridging phosphate oxygens.

Sugar Pucker Changes May Be Due to C41 and C75. The Raman spectra near 800 cm^{-1} are sensitive to changes in the phosphodiester backbone conformation. This region undergoes small and opposing changes when either Mg^{2+} or $Co(NH_3)_6^{3+}$ binds in HDV crystals. The data suggest that 2−3% of the linkages undergo a change in the ribose moiety when Mg^{2+} binds. In addition, the changes are in opposite directions for the two ions, with Mg^{2+} binding slightly increasing the C2′-endo and cobalt hexamine increasing the C3′-endo conformations (*27*, *28*, *34*).

Analysis of the cleaved structure of the ribozyme by MC-annotate (*42*) reveals that only two HDV ribozyme nucleotides are in the C2′-endo-anti conformation: C41 and C75. Moreover, both of these protonatable residues have been implicated as being near Mg^{2+} ions (*36*, *43*), consistent with appearance of these rare sugar puckers upon Mg^{2+} uptake. The crystal structure of the cleaved form of the ribozyme likely represents protonated C41 and deprotonated C75 (*36*, *44*). This is because C41 protonation couples favorably with Mg^{2+} binding,[5] while C75 couples unfavorably; moreover, the scissile phosphate is likely necessary for upward pK_a shifting of C75 and is absent in this structure. Together, these and other observations suggest that Mg^{2+} binding drives deprotonation of C75 and protonation of C41, both of which give rise to C2′-endo-anti conformations. Since there are 71 nt in our crystallographic construct, changes at these two residues could account for all of the ~3% observed signal intensity change.

Quantitative Analysis of Metal Ion and Proton Binding in the HDV Ribozyme: Comparison with Other Studies. Previous Raman crystallographic studies suggest that protonation of C75 and Mg^{2+} binding in the crystal form of the HDV ribozyme are similar in solution (*26*). For example, pK_a values of 6.15 and 6.4 in the presence of 20 and 2 mM Mg^{2+} measured for catalytic C75 in the crystal (*24*) are consistent with solution pK_as of 6.1 and 6.5 in 10 and 1.9 mM Mg^{2+} (*3*), respectively. Here, we found that the pH 7.0 inhibition constant for $Co(NH_3)_6^{3+}$ ($K_{i,Co(NH_3)_6^{3+}}$) and dissociation constant ($K_{D,Mg^{2+}}$) for Mg^{2+} are 47 μM and 1.7 mM in the crystal, in good agreement with values of 45 μM and 2.4 mM in solution (Table 2) (*3*). In addition, the Hill values for Mg^{2+} binding are in agreement in the crystal and solution with values of 1.5 and 1.4, respectively (Table 2). These data strongly support metal ion binding behavior in the crystal being essentially the same as in solution.

The Hill coefficient for Mg^{2+} binding obtained by measuring deprotonation of C75 as a function of Mg^{2+} concentration was determined to be 8.0 ± 1.6 (Figure 3). This number differs from the Hill coefficient determined by examining the dependence of the rate constant for chemistry on the Mg^{2+} concentration (*3*). It is has been noted, however, that a Hill coefficient >1 may not reflect the true number of metal binding sites (*45*). One possibility is that binding of the structural and catalytic ions is accompanied by the 5−6 additional ions observed in crystal structures of the ribozyme. Such ions could be silent to functional experiments in solution, which is consistent with their occupancy of non active site regions of the ribozyme such as within the major grooves of double helices.

Binding of either Mg^{2+} or $Co(NH_3)_6^{3+}$ Induces Deprotonation of C75. Solution kinetic studies indicate that the proton on C75 binds anticooperatively with a magnesium ion in the HDV ribozyme active site. In our previous characterization of the pK_a of C75, this is revealed as a shift of the pK_a of C75 toward neutrality as the magnesium ion concentration is reduced. In the present study, we observe related effects.

Introduction of the magnesium ion to the HDV ribozyme active site induces deprotonation of C75. At pH 6.0, binding of

[5]Protonation of C41 is likely invisible to the Raman features observed for CMP and C75. This is because C41, but not C75 or CMP, engages in extensive base pairing when it protonates.

≥10 mM Mg^{2+} (Figure 3) results in net gain of approximately one-half of a neutral cytosine. Since this pH is close to the measured pK_a of C75 and C75 is the only protonatable cytosine in this pH range, we interpret this finding in terms of protonation/deprotonation of the active site cytosine. As with the previous study, the values obtained by Raman crystallography agree with values obtained by kinetics studies in solution, suggesting that the conformation of the ribozyme in the crystal is relevant to the conformation of the ribozyme in solution.

In contrast to Mg^{2+} binding, introduction of $Co(NH_3)_6^{3+}$ to the HDV ribozyme is inhibitory; thus, it is difficult to measure the effects of this ion on pK_a using solution kinetic methods. As Raman spectroscopy does not depend on ribozyme activity for readout, we used it to ask whether $Co(NH_3)_6^{3+}$ and Mg^{2+} have similar effects on the pK_a of C75. As observed in Figure 4, binding of $Co(NH_3)_6^{3+}$ to the HDV ribozyme induces cytosine deprotonation. These data suggest that one of the binding sites for $Co(NH_3)_6^{3+}$ is within the HDV ribozyme active site such that the metal ion and the proton on C75 interact by electrostatic repulsion.

Structural Basis for $Co(NH_3)_6^{3+}$ Inhibition of the HDV Ribozyme. A unique characteristic of the HDV ribozyme is its inhibition by $Co(NH_3)_6^{3+}$ ions. While many of the small ribozymes fold and function in the absence of Mg^{2+} and presence of high concentrations of monovalent cations, and the hairpin ribozyme functions in the presence of $Co(NH_3)_6^{3+}$ (*12*, *13*), the HDV ribozyme is strongly inhibited by this $Mg(H_2O)_6^{2+}$ mimic. Binding of $Co(NH_3)_6^{3+}$ to the HDV ribozyme has been shown to be tight ($K_{i,Co(NH_3)_6^{3+}}$ ~45 μM) and competitive with $Mg(H_2O)_6^{2+}$ ($K_{D,Mg^{2+}}$ ~2.4 mM) (*3*). There are two models by which $Co(NH_3)_6^{3+}$ could have this effect on ribozyme activity: model 1, in which there are overlapping binding sites for $Co(NH_3)_6^{3+}$ and catalytic Mg^{2+}, or model 2, in which $Co(NH_3)_6^{3+}$ induces inhibitory conformational changes.

In favor of model 1, there is significant evidence that supports overlapping binding sites for $Co(NH_3)_6^{3+}$ and $Mg(H_2O)_x^{2+}$ ($x \leq 5$) within the HDV ribozyme active site. Raman data provide direct evidence for displacement of inner sphere Mg^{2+} by $Co(NH_3)_6^{3+}$, and binding of $Co(NH_3)_6^{3+}$ and $Mg(H_2O)_x^{2+}$ both induce deprotonation of C75. Thus, both of these ions are bound within the HDV ribozyme active site in proximity to C75. In addition, there is evidence that the inner sphere Mg^{2+} displaced by $Co(NH_3)_6^{3+}$ is bound to a guanosine N7, and we have previously demonstrated that an $Mg(H_2O)_x^{2+}$ ion is bound to the N7 of G1. Finally, solution biochemical data have demonstrated that $Co(NH_3)_6^{3+}$ inhibits the HDV ribozyme by binding competitively with Mg^{2+} (*3*). Thus, solution and Raman crystallographic data are both consistent with a model in which $Co(NH_3)_6^{3+}$ inhibits the HDV ribozyme by displacing the active site $Mg(H_2O)_x^{2+}$ bound to G1. It is noteworthy that Been et al. (*46*) also suggested the possibility of the replacement of the inner sphere coordinated catalytic Mg^{2+} by $Co(NH_3)_6^{3+}$ due to the flexibility of HDV ribozyme active site.

Nevertheless, there is also support for model 2, in which $Co(NH_3)_6^{3+}$ inhibits the HDV ribozyme by inducing a conformational change upon displacing Mg^{2+} ions and stabilizing an inactive conformation of the ribozyme. Small conformational changes could play a critical role in positioning functional groups for the in-line attack during catalysis. Such a mechanism has been observed in the hammerhead ribozyme wherein lanthanides stabilize a ground-state, nonfunctional conformation of the ribozyme (*47*). Indeed, we have demonstrated that addition of Mg^{2+} or $Co(NH_3)_6^{3+}$ to the HDV ribozyme induces unique minor conformational changes of opposite effect and of unknown origin.

Of course, model 1 and model 2 are not mutually exclusive. Changes in activity may arise both from the ability of $Co(NH_3)_6^{3+}$ to displace inner sphere bound catalytic Mg^{2+} in HDV and from different conformations caused by Mg^{2+} and $Co(NH_3)_6^{3+}$ binding.

Finally, there is the observation that monovalent cations such as Na^+ support catalysis, albeit less efficiently than Mg^{2+}, while $Co(NH_3)_6^{3+}$ is inhibitory. If model 1 best describes the mechanism of $Co(NH_3)_6^{3+}$ inhibition, then activity with small monovalent ions may be related to their ability to directly coordinate to the N7 and provide an ordered water from their hydration shell for general base catalysis, as seen crystallographically with Tl^+ (*7*). However, if model 2 is correct, then monovalent ions may simply support an active fold similar to that seen in the presence of Mg^{2+}.

Clearly, it will take additional studies to fully understand roles of metal ions in the HDV ribozyme. Further, X-ray crystallographic analysis of the HDV ribozyme active site with a substrate analogue bound could provide deeper understanding of how metal ions bind within the active site. In addition, isotopic substitutions at the N7 of G1 and at specific phosphodiester bonds would allow Raman spectroscopy to follow these changes at the site-specific level.

ACKNOWLEDGMENT

We thank Mike Harris and Eric Christian for sharing unpublished data.

SUPPORTING INFORMATION AVAILABLE

Derivations of eqs 1−3 and analysis of competitive binding of $Co(NH_3)_6^{3+}$ and Mg^{2+} in the HDV ribozyme when Hill coefficient is held to 2 (Figure S1). This material is available free of charge via the Internet at http://pubs.acs.org.

REFERENCES

1. Suh, Y. A., Kumar, P. K., Taira, K., and Nishikawa, S. (1993) Self-cleavage activity of the genomic HDV ribozyme in the presence of various divalent metal ions. *Nucleic Acids Res. 21*, 3277–3280.
2. Shih, I. H., and Been, M. D. (1999) Ribozyme cleavage of a 2,5-phosphodiester linkage: mechanism and a restricted divalent metal-ion requirement. *RNA 5*, 1140–1148.
3. Nakano, S., Chadalavada, D. M., and Bevilacqua, P. C. (2000) General acid-base catalysis in the mechanism of a hepatitis delta virus ribozyme. *Science 287*, 1493–1497.
4. Nakano, S., Proctor, D. J., and Bevilacqua, P. C. (2001) Mechanistic characterization of the HDV genomic ribozyme: assessing the catalytic and structural contributions of divalent metal ions within a multichannel reaction mechanism. *Biochemistry 40*, 12022–12038.
5. Nakano, S., Cerrone, A. L., and Bevilacqua, P. C. (2003) Mechanistic characterization of the HDV genomic ribozyme: classifying the catalytic and structural metal ion sites within a multichannel reaction mechanism. *Biochemistry 42*, 2982–2994.
6. Perrotta, A. T., and Been, M. D. (2006) HDV ribozyme activity in monovalent cations. *Biochemistry 45*, 11357–11365.
7. Ke, A., Ding, F., Batchelor, J. D., and Doudna, J. A. (2007) Structural roles of monovalent cations in the HDV ribozyme. *Structure 15*, 281–287.
8. Gong, B., Chen, Y. Y., Christian, E. L., Chen, J. H., Chase, E., Chadalavada, D. M., Yajima, R., Golden, B. L., Bevilacqua, P. C., and Carey, P. R. (2008) Detection of inner-sphere interactions between magnesium hydrate and the phosphate backbone of the HDV ribozyme using Raman crystallography. *J. Am. Chem. Soc. 130*, 9670–9672.

9. Chen, J. H., Gong, B., Bevilacqua, P. C., Carey, P. R., and Golden, B. L. (2009) A catalytic metal ion interacts with the cleavage site G·U wobble in the HDV ribozyme. *Biochemistry 48*, 1498–1507.
10. Wadkins, T. S., Shih, I., Perrotta, A. T., and Been, M. D. (2001) A pH-sensitive RNA tertiary interaction affects self-cleavage activity of the HDV ribozymes in the absence of added divalent metal ion. *J. Mol. Biol. 305*, 1045–1055.
11. Cerrone-Szakal, A. L., Siegfried, N. A., and Bevilacqua, P. C. (2008) Mechanistic characterization of the HDV genomic ribozyme: solvent isotope effects and proton inventories in the absence of divalent metal ions support C75 as the general acid. *J. Am. Chem. Soc. 130*, 14504–14520.
12. Hampel, A., and Cowan, J. A. (1997) A unique mechanism for RNA catalysis: the role of metal cofactors in hairpin ribozyme cleavage. *Chem. Biol. 4*, 513–517.
13. Nesbitt, S., Hegg, L. A., and Fedor, M. J. (1997) An unusual pH-independent and metal-ion-independent mechanism for hairpin ribozyme catalysis. *Chem. Biol. 4*, 619–630.
14. Young, K. J., Gill, F., and Grasby, J. A. (1997) Metal ions play a passive role in the hairpin ribozyme catalysed reaction. *Nucleic Acids Res. 25*, 3760–3766.
15. Duguid, J., Bloomfield, V. A., Benevides, J., and Thomas, G. J., Jr. (1993) Raman spectroscopy of DNA-metal complexes. I. Interactions and conformational effects of the divalent cations: Mg, Ca, Sr, Ba, Mn, Co, Ni, Cu, Pd, and Cd. *Biophys. J. 65*, 1916–1928.
16. Duguid, J. G., Bloomfield, V. A., Benevides, J. M., and Thomas, G. J., Jr. (1995) Raman spectroscopy of DNA-metal complexes. II. The thermal denaturation of DNA in the presence of Sr^{2+}, Ba^{2+}, Mg^{2+}, Ca^{2+}, Mn^{2+}, Co^{2+}, Ni^{2+}, and Cd^{2+}. *Biophys. J. 69*, 2623–2641.
17. Wang, J. H., Xiao, D. G., Deng, H., Callender, R., and Webb, M. R. (1998) Vibrational study of phosphate modes in GDP and GTP and their interaction with magnesium in aqueous solution. *Biospectroscopy 4*, 219–227.
18. Langlais, M., Tajmir-Riahi, H. A., and Savoie, R. (1990) Raman spectroscopic study of the effects of Ca^{2+}, Mg^{2+}, Zn^{2+}, and Cd^{2+} ions on calf thymus DNA: binding sites and conformational changes. *Biopolymers 30*, 743–752.
19. Ahmad, R., Arakawa, H., and Tajmir-Riahi, H. A. (2003) A comparative study of DNA complexation with Mg(II) and Ca(II) in aqueous solution: major and minor grooves bindings. *Biophys. J. 84*, 2460–2466.
20. Moller, M. R., Bruck, M. A., O'Connor, T., Armatis, F. J., Knolinski, E. A., Kottmair, N., and Tobias, R. S. (1980) Heavy metal -nucleotide interactions. 14. Raman difference spectrophotometric studies of competitive reactions in mixtures of four nucleotides with electrophiles. Factors governing selectivity in the binding reactions. *J. Am. Chem. Soc. 102*, 4589–4598.
21. O'Connor, T., Bina, M., McMillin, D. R., Haley, M. R., and Tobias, R. S. (1982) Heavy metal-nucleotide interactions. 15. Reactions of calf thymus DNA with the electrophiles methylmercury(II) nitrate, cis-dichlorodiammineplatinum(II), and trans-dichlorodiammineplatinum(II) studied using Raman difference spectroscopy. Evidence for the formation of C-DNA upon metalation. *Biophys. Chem. 15*, 223–234.
22. Callender, R., and Deng, H. (1994) Nonresonance Raman difference spectroscopy: a general probe of protein structure, ligand binding, enzymatic catalysis, and the structures of other biomacromolecules. *Annu. Rev. Biophys. Biomol. Struct. 23*, 215–245.
23. Carey, P. R. (2006) Raman crystallography and other biochemical applications of Raman microscopy. *Annu. Rev. Phys. Chem. 57*, 527–554.
24. Gong, B., Chen, J. H., Chase, E., Chadalavada, D. M., Yajima, R., Golden, B. L., Bevilacqua, P. C., and Carey, P. R. (2007) Direct measurement of a pK(a) near neutrality for the catalytic cytosine in the genomic HDV ribozyme using Raman crystallography. *J. Am. Chem. Soc. 129*, 13335–13342.
25. Gong, B., Chen, J. H., Yajima, R., Chen, Y. Y., Chase, E., Chadalavada, D. M., Golden, B. L., Carey, P. R., and Bevilacqua, P. C. (2009) Raman crystallography of RNA, Methods (doi:10.1016/j.ymeth.2009.1004.1016).
26. Gong, B., Chen, J. H., Chase, E., Chadalavada, D. M., Yajima, R., Golden, B. L., Bevilacqua, P. C., and Carey, P. R. (2007) Direct measurement of a pK(a) near neutrality for the catalytic cytosine in the genomic HDV ribozyme using Raman crystallography. *J. Am. Chem. Soc. 129*, 13335–13342.
27. Thomas, G. J., Jr., and Tsuboi, M. (1993) Raman spectroscopy of nucleic acids and their complexes, in Advances in Biophysical Chemistry , pp 1−70.
28. Carey, P. R. (1982) Biochemical Application of Raman and Resonance Raman Spectroscopies , Academic Press, New York.
29. Lafleur, L., Rice, J., and Thomas, G. J., Jr. (1972) Raman studies of nucleic acids. VII. Poly A-poly U and poly G-poly C. *Biopolymers 11*, 2423–2437.
30. Fish, S. R., Hartman, K. A., Stubbs, G. J., and Thomas, G. J., Jr. (1981) Structural studies of tobacco mosaic virus and its components by laser Raman spectroscopy. *Biochemistry 20*, 7449–7457.
31. Small, E. W., and Peticolas, W. L. (1971) Conformational dependence of the Raman scattering intensities from polynucleotides. 3. Order-disorder changes in helical structures. *Biopolymers 10*, 1377–1418.
32. Majoube, M. (1984) Vibrational spectra of guanine. A noral coordinate analysis. *J. Chim. Phys. 81*, 303–315.
33. Moller, M. R., Bruck, M. A., O'Connor, T., Armatis, F. J., Jr., Knolinski, E. A., Kottmair, N., and Tobias, R. S. (1980) Heavy metal-nucleotide interactions. 14. Raman difference spectrophotometric studies of competitive reactions in mixtures of four nucleotides with the electrophiles methylmercury(II) perchlorate, cis dimethylgold(III) perchlorate, dichloroethylene-diamine-palladium(II), trans-dichlorodiaminepalladium(II), and aquopentaaminecobalt(III) perchlorate. Factors governing selectivity in the binding reactions. *J. Am. Chem. Soc. 102*, 4589–4598.
34. Rodriguez-Casado, A., Bartolome, J., Carreno, V., Molina, M., and Carmona, P. (2006) Structural characterization of the 5′ untranslated RNA of hepatitis C virus by vibrational spectroscopy. *Biophys. Chem. 124*, 73–79.
35. Hobro, A. J., Rouhi, M., Blanch, E. W., and Conn, G. L. (2007) Raman and Raman optical activity (ROA) analysis of RNA structural motifs in domain I of the EMCV IRES. *Nucleic Acids Res. 35*, 1169–1177.
36. Ferre-D'Amare, A. R., Zhou, K., and Doudna, J. A. (1998) Crystal structure of a hepatitis delta virus ribozyme. *Nature 395*, 567–574.
37. Ke, A., Zhou, K., Ding, F., Cate, J. H., and Doudna, J. A. (2004) A conformational switch controls hepatitis delta virus ribozyme catalysis. *Nature 429*, 201–205.
38. Jou, R., and Cowan, J. A. (1991) Ribonuclease H activation by inert transition-metal complexes. Mechanistic probes for metallocofactors: insights on the metallobiochemistry of divalent magnesium ion. *J. Am. Chem. Soc. 113*, 6685–6686.
39. Duffy, T. H., and Nowak, T. (1985) ^{1}H and ^{31}P relaxation rate studies of the interaction of phosphoenolpyruvate and its analogues with avian phosphoenolpyruvate carboxykinase. *Biochemistry 24*, 1152–1160.
40. Draper, D. E. (2004) A guide to ions and RNA structure. *RNA 10*, 335–343.
41. Draper, D. E. (2008) RNA folding: thermodynamic and molecular descriptions of the roles of ions. *Biophys. J. 95*, 5489–5495.
42. http://www-lbit.iro.umontreal.ca/mcannotate-simple.
43. Nakano, S., and Bevilacqua, P. C. (2007) Mechanistic characterization of the HDV genomic ribozyme: a mutant of the C41 motif provides insight into the positioning and thermodynamic linkage of metal ions and protons. *Biochemistry 46*, 3001–3012.
44. Ferre-D'Amare, A. R., and Doudna, J. A. (2000) Crystallization and structure determination of a hepatitis delta virus ribozyme: use of the RNA-binding protein U1A as a crystallization module. *J. Mol. Biol. 295*, 541–556.
45. Weiss, J. N. (1997) The Hill equation revisited: uses and misuses. *FASEB J. 11*, 835–841.
46. Shih, I. H., and Been, M. D. (2002) Catalytic strategies of the hepatitis delta virus ribozymes. *Annu. Rev. Biochem. 71*, 887–917.
47. Feig, A. L., Scott, W. G., and Uhlenbeck, O. C. (1998) Inhibition of the hammerhead ribozyme cleavage reaction by site-specific binding of Tb. *Science 279*, 81–84.